Numerical calculation of steady-state skin effect problems in axisymmetry

Qi Sheng Huang, Laurent Krähenbühl, Alain Nicolas

NUMERICAL CALCULATION OF STEADY-STATE SKIN EFFECT PROBLEMS IN AXISYMMETRY

Q.S. Huang, L. Krahenbuhl, A. Nicolas

Département d'Electrotechnique
Unité Associée au C.N.R.S. No 829
Ecole Centrale de Lyon
BP 163 - 69131 ECULLY CEDEX - FRANCE

ABSTRACT

A numerical method based upon the boundary element method is described to solve steady-state skin effect problems in axisymmetry. This method can be used to treat problems with very small skin depth.

The program realised is designed for engineers' assistance, so special attention has been paid to accuracy and validation. Besides current density distribution which is graphicaly displayed, all global magnitudes can be immediately obtained as final results from the program.

1. INTRODUCTION

The distribution of eddy currents in induction problems is very difficult to be calculated by the finite element method when the skin depth (which is determined by resistivity, permeability and excitating frequency) is very small.

In this paper a numerical method suitable for this problem in axisymmetry based upon the boundary element method (BEM) is described. It retains all the advantages of the BEM and avoids surface integration of the source term.

2. THE BOUNDARY INTEGRAL FORMULATION

The formulation of the vector and scalar potential A-ϕ is adapted to model the problem:

$$\vec{B} = \overrightarrow{rot}\ \vec{A}$$
$$\vec{E} = -\partial\vec{A}/\partial t + \overrightarrow{grad}\ \phi \qquad (1)$$

Assuming that permeability μ is constant, we obtain [2]:

$$\Delta\vec{A} - j\mu\sigma\omega\vec{A} = -\mu\vec{J}ex \qquad (2)$$

where:

$\vec{J}ex$: exciting current density
σ : conductivity of the conductor
$\omega/2\pi$: frequency which will produce the skin effect.

The second Green's identity permits to write (2) as [1]:

$$C_p\vec{A}(P) = -\int_\Sigma \left(\vec{A}\frac{\partial G}{\partial n} - G\frac{\partial\vec{A}}{\partial n}\right)ds - \mu\int_V \vec{J}_{ex}\,G\,dv \qquad (3)$$

where:

$G = e^{-j\lambda r}/4\pi r$
r : distance between point P and the current point of integration
$\lambda^2 = -j\mu\sigma\omega$
Σ : boundary of the region V
Cp : solid angle viewing Σ from the point P

In axisymmetry, the potential A has only one component, so equation (3) becomes:

$$C_pA(P) = -\int_\Sigma \left(\cos\varphi\, A\frac{\partial G}{\partial n} - \cos\varphi\, G\frac{\partial A}{\partial n}\right)ds - \mu\int_V J_{ex}\cos\varphi\, G\,dv \qquad (4)$$

It can be demonstrated that:

$$\frac{\partial A}{\partial n} = \mu_r\Psi - \cos\alpha\frac{A}{R} \qquad (5)$$

where:

$\Psi/\mu_0 = -Ht$

Ht : tangential component of the magnetic field, continuous through the interface of different media.

φ, α and R are defined in the following figure:

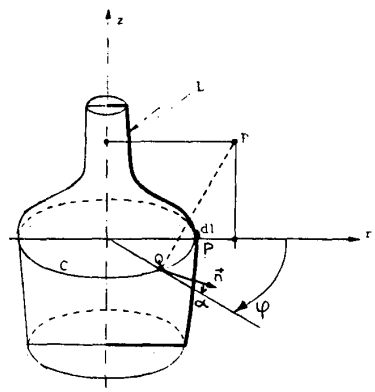

Figure 1: Typical axisymmetric problem

0018-9464/88/0100-0201$01.00©1988 IEEE

Using the relation (5) in equation (4), the number of unknowns can be reduced and the interface condition (continuity of the normal component of the flux density and of the tangential components of the magnetic field) is implicitly assured.

The weighting functions G and $\partial G/\partial n$ depend only on the geometry: equation (4) can be written as:

$$C_p A(p) = -\int_L \left[A\left(G'_{ax} + \frac{\cos\alpha}{R} G_{ax}\right) - \mu_i \Psi G_{ax} \right] dl - \mu \int_V J_{ex} \cos\varphi \, G \, dv \qquad (6)$$

where:

$$G_{ax} = \int_C \cos\varphi \; G \, dc \qquad G'_{ax} = \int_C \cos\varphi \; \frac{\partial G}{\partial n} \, dc \qquad (7)$$

3. TRANSFORMATION OF VOLUME INTEGRAL OF THE SOURCE

Because of the axisymmetry of the inductor, the volume integral in (6) is reduced to the surface integral:

$$\mu \int_V J_{ex} \cos\varphi \, G \, dv = 2\pi \int_S \left(J_{ex} \int_0^{\pi} R \cos\varphi \, G \, d\varphi \right) dR \, dZ \qquad (8)$$

where S is the section of the exciting coil (see figure 2).

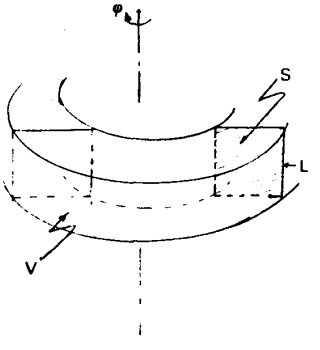

- Figure 2 -

Using the hypothesis that Jex is constant over the section of the exciting coil and that the eddy current is negligible in the exciting coil (these are well verified when the wire section is very small vis-à-vis the dimension of the problem), the surface integration in (8) can be translated as an one dimensional integral:

$$\mu \int_V J_{ex} \cos\varphi \, G \, dv = 2\pi J_{ex} \int_L N \, dZ \qquad (9)$$

with:

$$N = \frac{1}{4\pi} \int_0^{\pi} \cos\varphi \left[r + R_p \cos\varphi \, \ln\left(R - R_p \cos\varphi + r\right) \right] d\varphi \qquad (10)$$

This transformation facilitates the geometry description and numerical calculation of this term.

4. THE KERNEL CALCULATIONS

In (6), G_{ax} and G'_{ax} are called the kernels of the boundary integral. Because the function G has a singular point (for $r = 0$), the integrals (8) are non-proper, some precautions must be taken in the numerical calculation of the kernels.

For the non-conducting region, the function G becomes:

$$G = 1/4\pi r \qquad (11)$$

so it is convenient to write (6) as:

$$G_{ax} = \int_C \cos\varphi \; G_1 dc + \int_C \cos\varphi \; G_2 dc = G_{ax1} + G_{ax2} \qquad (12)$$

$$G'_{ax} = \int_C \cos\varphi \frac{\partial G_1}{\partial n} dc + \int_C \cos\varphi \frac{\partial G_2}{\partial n} dc = G'_{ax1} + G'_{ax2}$$

with:

$$G_1 = \frac{1}{4\pi r} \qquad G_2 = \frac{e^{-\lambda r} - 1}{4\pi r} \qquad (13)$$

$G_2(r)$ is well defined for every value of the variable r, so G_{ax2} and G'_{ax2} can be directly obtained by numerical integral.

It can be derived as:

$$G_{ax1} = \frac{R}{\pi D} \int_0^{\pi/2} \frac{2\sin^2\theta - 1}{\sqrt{1 - k^2 \sin^2\theta}} \, d\theta = \frac{R}{\pi D} \left[\frac{-2}{k^2} E(k^2) + \left(\frac{2}{k^2} - 1 \right) K(k^2) \right] \qquad (14)$$

with:

$k^2 = 4.r.R/D^2$

D : as shown in figure 3

K, E : complete elliptic integral of first and second kind [3]

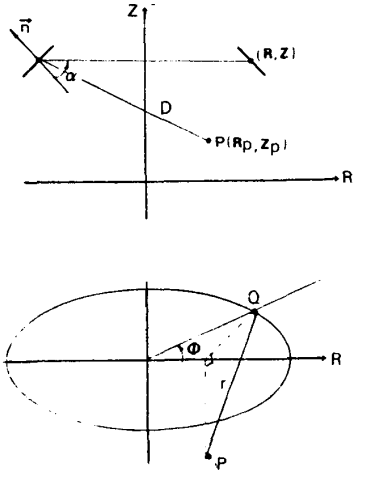

- Figure 3 -

The numerical calculation of integrals K and E can be easily done in several ways [1]. G_{ax1} can also be expressed in the similar way.

By using the isoparametric finite elements for boundary discretization, one obtains:

$$C_p A(P) = \sum_k \left[\sum_i \left(A_{ki}\, d_{ki} - \mu_r \Psi_{ki}\, b_{ki} \right) - 2\mu J_{ex}\, e_k \right] \quad (15)$$

with:

$$d_{ki} = -\int_{-1}^{1} P_i(u)\, J_k(u)\, G_{ax} + \frac{\cos\alpha}{R}\, G_{ax}\, J_k(u)\, du$$

$$b_{ki} = -\int_{-1}^{1} P_i(u)\, G_{ax}\, J_k(u)\, du \quad (16)$$

$$e_k = \int_{-1}^{1} N \frac{\partial Z}{\partial u}\, du$$

where:

- k : subscript of the boundary finite elements
- i : subscript of the weighting functions
- P(u) : weighting function
- J(u) : jacobien (dl = J(u).du)
- A_{ki}, Ψ_{ki}: values of A and Ψ at the discrete point of finite elements

5. VALIDATION

The program that we have realised is designed for engineers assistance, the validation has been done in several ways:

5.1 Experiment:

The dissipating power of steady-state eddy current in a block of cylindrical metal is measured under different excitation frequencies and is compared with the results calculated by our program. Figure 4 shows the experimental system. We have used a digital wattmeter whose accuracy is 0.5% for the frequency range 10Hz-1KHz.

The dimension of the sample and the boundary discretization are illustrated in figure 5. Figure 6 shows the distribution of the induction lines resulting from the numerical calculation.

The comparision of the calculated results with the measurement proves the good precision of the numerical calculation, in spite of the large discrete elements. The differences in active power is less than 5% (see table 1).

f [Hz]	100	300	500	800	1000
P [W] (measured)	0.09	0.196	0.295	0.36	0.41
P [W] (computed)	0.0919	0.1968	0.2804	0.357	0.406

- Table 1 -

5.2 Comparision with the finite element method:

The program ACDC [2] based upon the finite element method is already used by industries. We use it as a reference for the calculation low frequences. The results of the potential A calculated by the two programs are almost identical.

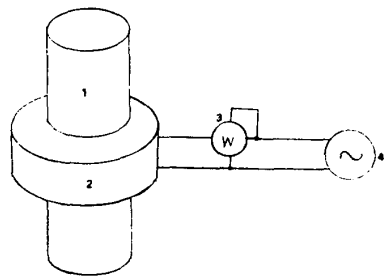

Figure 4: The experimental system
1: Charge 2: Inductor
3: Wattmeter 4: Source

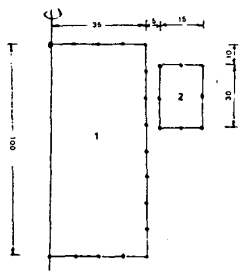

Figure 5: The dimensions of the sample and the boundary discretization

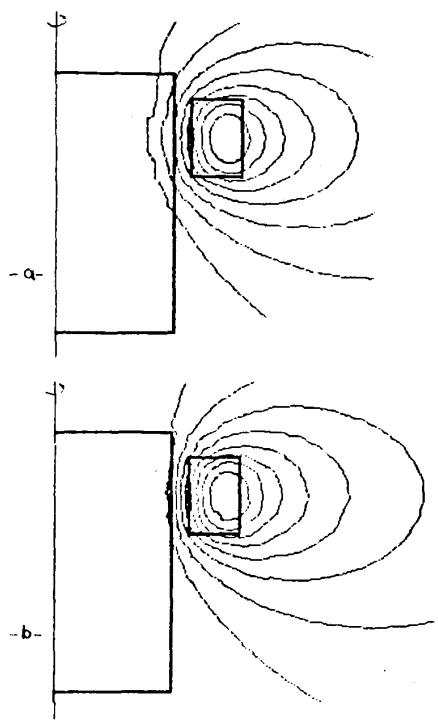

Figure 6: The induction lines
a : f = 100Hz
b : f = 1kHz

5.3 Indirect validation for high frequency:

For high frequency, the skin depth is very small, ACDC can't be used and the power factor $\cos\phi$ is very bad, neither the measurement can be used for validation.

When the skin depth tends to zero, it can be shown that the phase angle of the complex dissipating power tends to 45°, so we use it as a reference for the validation in high frequence.

The results are in table 2. It can be seen that the validation is proved.

f [kHz]	0.1	0.5	1.0	3.0	6.0
skin depth [mm]	12.2	5.46	3.858	2.228	1.575
θ [°]	51.45	49.1	47.89	46.7	45.6

- Table 2 -

6. CONCLUSION

The program realised gives excellent results. It needs a very short geometry description time. Besides current density distribution, all global magnitudes can be immediatly obtained as final results from the program.

But it can't treate the saturation phenomenon. Although it has been shown that the BEM is applicable for some weakly non-linear problems by an iterative solution[4], the non-linear terms are treated as forcing functions and it is necessary to subdivide the saturable regions into finite elements. When the skin depth is very small, we meet the same difficulty as in the finite element method.

- REFERENCES -

[1] L. Krahenbuhl and A. Nicolas: "Axisymmetric formulation for boundary integral equation methods in scalar potential problem" - IEEE T-MAG 19/6, 2364-2366, November 1983 -

[2] C. Marchand and A. Foggia "2D finite elements program for magnetic indution heating" - IEEE T-MAG 19/6, 2647-2649, November 1983 -

[3] M. Abramowitz and A. Stegun: "Handbook of mathematical functions" - Dover Publication -

[4] C.A. Brebbia and S. Walker: "Boundary element techniques in engineering" - Newnes Butterworths 1980 -